Nuclear Structure Notes on Element 115 Decay Chains

Rudolph, Dirk; Sarmiento, Luis; Forsberg, Ulrika

Published in:
AIP Conference Proceedings

DOI:
10.1063/1.4932259

2015

Nuclear structure notes on element 115 decay chains

D. Rudolph, L. G. Sarmiento, and U. Forsberg

Citation: AIP Conference Proceedings **1681**, 030015 (2015); doi: 10.1063/1.4932259
View online: http://dx.doi.org/10.1063/1.4932259
View Table of Contents: http://scitation.aip.org/content/aip/proceeding/aipcp/1681?ver=pdfcov
Published by the AIP Publishing

Nuclear Structure Notes on Element 115 Decay Chains

D. Rudolph[1,a)], L.G. Sarmiento[1] and U. Forsberg[1]

[1]*Department of Physics, Lund University, 22100 Lund, Sweden*

[a)]Corresponding author: Dirk.Rudolph@nuclear.lu.se

Abstract. Hitherto collected data on more than hundred α-decay chains stemming from element 115 are combined to probe some aspects of the underlying nuclear structure of the heaviest atomic nuclei yet created in the laboratory.

INTRODUCTION

"The quest for superheavy elements is driven by the desire to find and explore one of the extreme limits of existence of matter" [1]. More than 40 years ago, an island of stability of superheavy nuclei was predicted by nuclear structure theorists (see, e.g., Ref. [2]). This island rests on increased nuclear stability due to anticipated magic proton and neutron numbers at spherical nuclear shape (see, e.g., Ref. [3]), while surrounding archipelagos may also arise from increased nuclear binding of deformed atomic nuclei [4, 5]. Even today theoreticians face the challenge – or have the freedom – to extrapolate over several tens of mass units towards the island, based on quite reliable spectroscopic information in the region around nobelium and rutherfordium [6].

Along their way, experimentalists have not only been producing heavier and heavier atomic nuclei, but also added more and more chemical elements to the Periodic Table. Present-day research builds upon one-atom-at-a-time creation and observation. In this context, 'time' refers to typically a day, a week, or as much as several months – and it is at this tiny rate that detailed spectroscopic information needs to be obtained.

During the past 15 years, correlated α-decay chains have been observed in a number of experiments performed at the Flerov Laboratory of Nuclear Reactions (FLNR) in Dubna, Russia. Beams of ^{48}Ca (Z = 20) impinged on actinide targets (Z = 92-98). The decay chains were interpreted to start from isotopes of elements Z = 112-118, produced via the mechanism of fusion-evaporation reactions [7, 8]. The α-decays of nuclei with even proton number, Z, and even mass number, A, typically proceed from ground-state to ground-state. The decay energies along such decay chains are thus characteristic for a given decay step and can be used as a fingerprint for a given isotope of a certain element [9].

Decay patterns are usually much more complex for α decays of odd-A or especially odd-odd nuclei. Their α decays usually proceed to excited states in the daughter nucleus [10]. On the one hand, decay into excited states hampers *indirect* methods of determining Z, not least because decay chains along the same isotopes may follow different decay paths depending on the starting point of a certain isotopic decay sequence. On the other hand, the possibility arises to observe X-ray photons in the course of electromagnetic internal conversion decays of the excited states in α-decay daughter nuclei [11]. X-ray energies are predicted with high precision even for the heaviest elements since long (see, e.g., Ref. [12]), and they are characteristic for a given proton, hence atomic, number [13]. In addition, high-resolution α-photon coincidence spectroscopy – such as pioneered on element Z = 115 decay chains – closes in towards nuclear structure studies near the island of stability [14].

Some nuclear structure assessments along element 115 decay chains are subject of these Proceedings.

CORRELATION TIMES OF ELEMENT 115 DECAY CHAINS

The first report on α-decay chains associated with element 115 originates from experiments conducted with the Dubna gas-filled recoil separator (DGFRS) at the Flerov Laboratory of Nuclear Reactions (FLNR) Dubna, Russia [15]. The decay data of in total 37 decay chains of element 115, which have been produced in the reaction ^{48}Ca+^{243}Am at

Nuclear Structure and Dynamics '15
AIP Conf. Proc. 1681, 030015-1–030015-6; doi: 10.1063/1.4932259

JINR-DGFRS since then, are summarized in Tables II-IV in Ref. [16]. A first high-resolution α-photon coincidence experiment was conducted at the gas-filled 'TransActinide Separator and Chemistry Apparatus' (TASCA) at the GSI Helmholtzzentrum für Schwerionenforschung, Darmstadt, Germany. Here, 30 decay chains were observed [14, 17] in less than three weeks in the TASISpec decay station [18, 19]. A similar experiment was performed shortly after using the Berkeley gas-filled separator (BGS) at Lawrence Berkeley National Laboratory (LBNL), United States, resulting in 46 element 115 decay chains and more α-photon coincidence events, thereby confirming the TASISpec data [20].

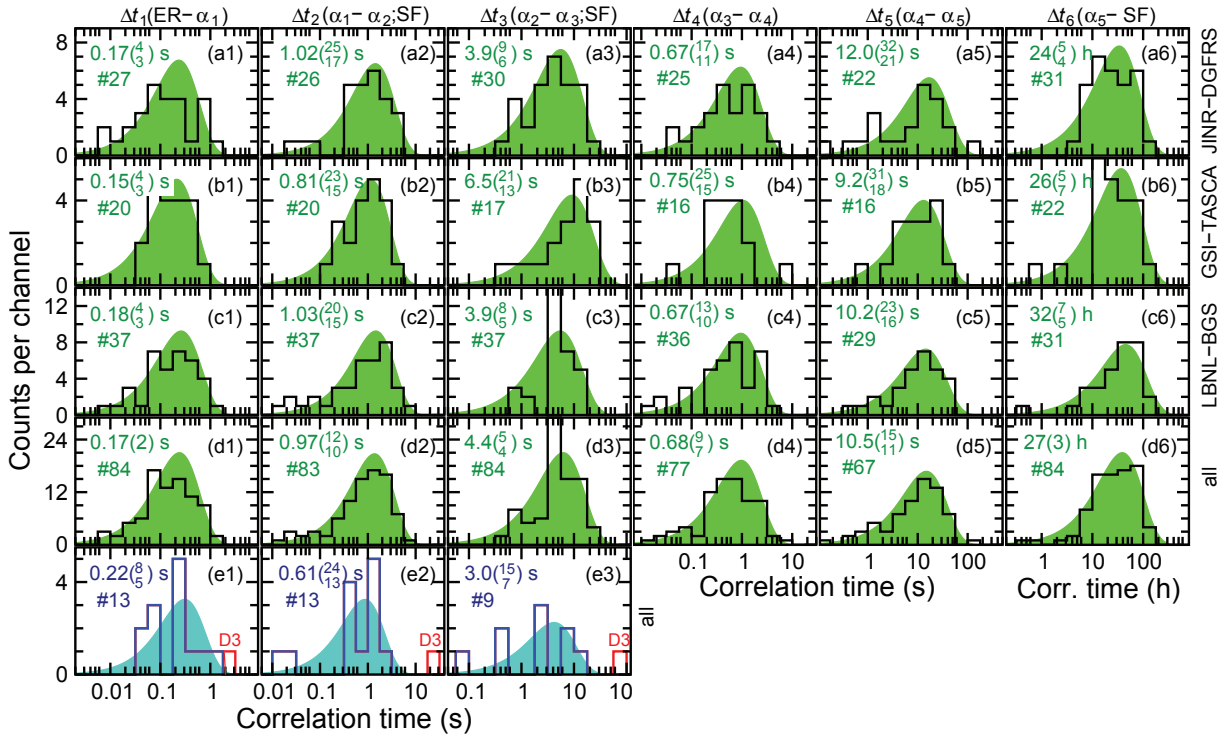

FIGURE 1. (Color online) Analysis of correlation times, Δt_i, of the up to six decay steps, $i = 1, ..., 6$, of element 115 decay chains. Rows (a), (b) and (c) provide data (black histograms) and corresponding half-life fit (shaded green areas) of the existing three data ensembles associated with $^{288}115$, taken at the DGFRS, TASCA and BGS facilities, respectively [14, 16, 20]. Row (d) shows the combination of all available data. Numbers behind the hash-tag, #, indicate the number of secure assignments used in the analysis. Row (e) provides the combined analysis of 13 (blue histograms and shaded turquoise areas) out of 14 so-called 'short' recoil-α-(α-)fission element 115 chains. The third chain of Table III in Ref. [16], denoted D3, is indicated in red, due to outstandingly long correlations times for *all three decay steps*.

Combining the three data sets, there are in total 113 decay chains of directly produced evaporation residues (ER) of element 115. The vast majority of these, namely 33+23+43=99 chains, comprise five subsequent α decays and a concluding spontaneous fission (SF). They are seemingly consistent with an interpretation of only one decay sequence each of the odd-A isotope $^{287}115$ (2+1+0=3 chains) and odd-odd $^{288}115$ (31+22+43=96 chains), respectively [14, 16, 20, 21, 22, 23]. Using only secure assignments and the minor modification of Table II in Ref. [16] as discussed in Ref. [14], Figure 1 shows the correlation times of the six decay steps of the 96 decay chains associated with $^{288}115$. The first three rows (a)-(c) correspond to separate DGFRS, TASCA, and BGS data, respectively, while row (d) shows the combined results. Due to a slight surplus of events, chains with $\Delta t_2 < 40$ ms may deserve special attention, though $Q_\alpha(^{284}113) = 10.0$ MeV and $T_{1/2}(^{284}113) = 100$ ms would imply an explanation for an unusually small hindrance factor, HF < 1 [24]. Furthermore, the 'Schmidt test' [25] does not call for the need of more than one decay sequence for any of the 24 ensembles in rows (a) to (d). Table 1 summarizes the corresponding numbers.

Next to this large amount of five-α-long decay chains, 0+2+2=4 short ER-α-SF chains and 4+5+1=10 ER-α-α-SF chains were observed in DGFRS, TASCA and BGS experiments, respectively. In conjunction with the recent TASCA and BGS data, it turns out that the assignment of these in total 14 chains to a certain isotope of element 115 is more complicated than anticipated for the by then only four chains observed at the DGFRS. The problem is

raised in Ref. [23], detailed in Ref. [17] and illustrated here in row (e) of Figure 1: Besides one DGFRS chain (named D3), which reveals exceptionally long correlation times in *all three decay steps*, these short chains have correlation times consistent with the 96 long chains associated with the decay of ^{288}115. Such an interpretation can readily be explained by, e.g., small SF (or electron capture, EC, followed by SF) branches at either ^{284}113 or ^{280}Rg. Of course, arguments on α-decay energies and excitation functions need to be considered as well, but on a chain-by-chain basis it is non-trivial and often impossible to decide whether any of these 13 chains starts from ^{288}115 or ^{289}115 [17].

TABLE 1. Half-lives, $T_{1/2}$, derived from the correlation times of different samples of decay data along element 115 decay chains. The number of data points and values $\sigma_{\Theta,\mathrm{exp}}$ as well as corresponding confidence interval $[\sigma_\mathrm{l}, \sigma_\mathrm{h}] = [\sigma_{\Theta,\mathrm{low}}, \sigma_{\Theta,\mathrm{high}}]$ (see Ref. [25]) are given. Based on Geant4 simulations [14, 20, 22, 26] but with a reservation for the presence of decay from isomeric excited states, Q_α values are provided for the combined data sets associated with ^{287}115 and ^{288}115. FWHM-type uncertainties of decay energies in Ref. [16] were divided by 2.35 to properly match 1σ-type uncertainties in Refs. [14, 20].

Ensemble	Quantity	Decay 115	Decay 113	Decay Rg	Decay Mt	Decay Bh	Decay Db
^{287}115, all	$T_{1/2}$	42($^{57}_{15}$) ms	82($^{199}_{34}$) ms	93($^{223}_{38}$) ms	21($^{28}_{8}$) ms	1.8($^{43}_{7}$) s	1.3($^{18}_{5}$) h
	#; $\sigma_{\Theta,\mathrm{exp}}$	3; 0.18 L	2; 0.38	2; 1.36	3; 0.54	2; 0.19	3; 0.79
	$[\sigma_\mathrm{l}, \sigma_\mathrm{h}]$	[0.19,1.91]	[0.04,1.83]	[0.04,1.83]	[0.19,1.91]	[0.04,1.83]	[0.19,1.91]
	Q_α (MeV)	10.78(3)	10.32(5)	10.53(5)	10.49(2)	9.45(6)	SF
^{288}115, [16]	$T_{1/2}$	0.17($^{4}_{3}$) s	1.02($^{25}_{17}$) s	3.9($^{9}_{6}$) s	0.67($^{17}_{11}$) s	12.0($^{32}_{21}$) s	24($^{5}_{4}$) h
	#; $\sigma_{\Theta,\mathrm{exp}}$	27; 1.39	26; 1.30	30; 1.01	25; 1.21	22; 1.61	31; 0.88 L
	$[\sigma_\mathrm{l}, \sigma_\mathrm{h}]$	[0.87,1.69]	[0.86,1.70]	[0.89,1.67]	[0.85,1.71]	[0.82,1.74]	[0.89,1.67]
[14]	$T_{1/2}$	0.15($^{4}_{3}$) s	0.81($^{23}_{15}$) s	6.5($^{21}_{13}$) s	0.75($^{25}_{15}$) s	9.2($^{31}_{18}$) s	26($^{7}_{5}$) h
	#; $\sigma_{\Theta,\mathrm{exp}}$	20; 0.85	20; 0.97	17; 1.08	16; 1.04	16; 1.01	22; 1.15
	$[\sigma_\mathrm{l}, \sigma_\mathrm{h}]$	[0.81,1.71]	[0.81,1.71]	[0.78,1.74]	[0.77,1.75]	[0.77,1.75]	[0.82,1.74]
[20]	$T_{1/2}$	0.18($^{4}_{3}$) s	1.03($^{20}_{15}$) s	3.9($^{8}_{5}$) s	0.67($^{13}_{10}$) s	10.2($^{23}_{16}$) s	32($^{7}_{5}$) h
	#; $\sigma_{\Theta,\mathrm{exp}}$	37; 1.63	37; 1.58	37; 0.73 L	36; 1.36	29; 1.22	31; 1.21
	$[\sigma_\mathrm{l}, \sigma_\mathrm{h}]$	[0.93,1.63]	[0.93,1.63]	[0.93,1.63]	[0.92,1.64]	[0.88,1.68]	[0.89,1.67]
all	$T_{1/2}$	0.17(2) s	0.97($^{12}_{10}$) s	4.4($^{5}_{4}$) s	0.68($^{9}_{7}$) s	10.5($^{15}_{11}$) s	27(3) h
	#; $\sigma_{\Theta,\mathrm{exp}}$	84; 1.41	83; 1.37	84; 0.93 L	77; 1.25	67; 1.32	84; 1.09
	$[\sigma_\mathrm{l}, \sigma_\mathrm{h}]$	[1.05,1.51]	[1.04,1.52]	[1.05,1.51]	[1.03,1.53]	[1.02,1.54]	[1.05,1.51]
	Q_α (MeV)	10.7(1)	10.2(1)	10.16(1)	10.10(1)	9.21(1)	SF
'Short', all*	$T_{1/2}$	0.22($^{8}_{5}$) s	0.61($^{24}_{13}$) s	3.0($^{15}_{7}$) s			
	#; $\sigma_{\Theta,\mathrm{exp}}$	13; 1.04	13; 1.50	9; 1.59			
	$[\sigma_\mathrm{l}, \sigma_\mathrm{h}]$	[0.72,1.77]	[0.72,1.77]	[0.62,1.84]			

* The third chain of Table III in Ref. [16], denoted D3, is excluded. For more details, see Ref. [17] and text.

DECAY ENERGIES, COINCIDENCES, GEANT4 AND DECAY SCHEMES

In the following, the first three decay steps of the 96 five-α-long decay chains associated with the production of ^{288}115 are discussed in some more detail. In line with panels (d1)-(d3) in Figure 1, panels (a)-(c) of Figure 2 provide the corresponding combination of decay-energy measurements of the three data ensembles taken at the DGFRS [16], with TASISpec [14, 17], and at the BGS [20]. Several notes are necessary. First of all, the decay energy measured in a certain pixel [14, 20, 17] or area [16] of the silicon implantation detector can be the sum of α-particle and conversion-electron contributions, in case the α decay proceeds into excited states of the daughter nucleus [cf. Figure 2(e)-(g)]. Secondly, one has to distinguish between so-called

- full-energy events; the α particle (and heavy recoiling daughter) left the complete energy in the implantation detector. This corresponds to typically ~ 50 % of the cases, and the precision of the measurement depends on the quality and long-term stability of the implantation detector.
- reconstructed events; the α particle left the implantation detector but is stopped in one of the upstream silicon box detectors. This happens in ~ 30-35 % of the cases. Energy precision is very much dependent on the control of emission angle, i.e. the pixelation of the upstream detector system, and knowledge of dead-layer thicknesses.
- escape events: the α particle left the implantation detector. These events are irrelevant for decay energy hence decay scheme considerations.

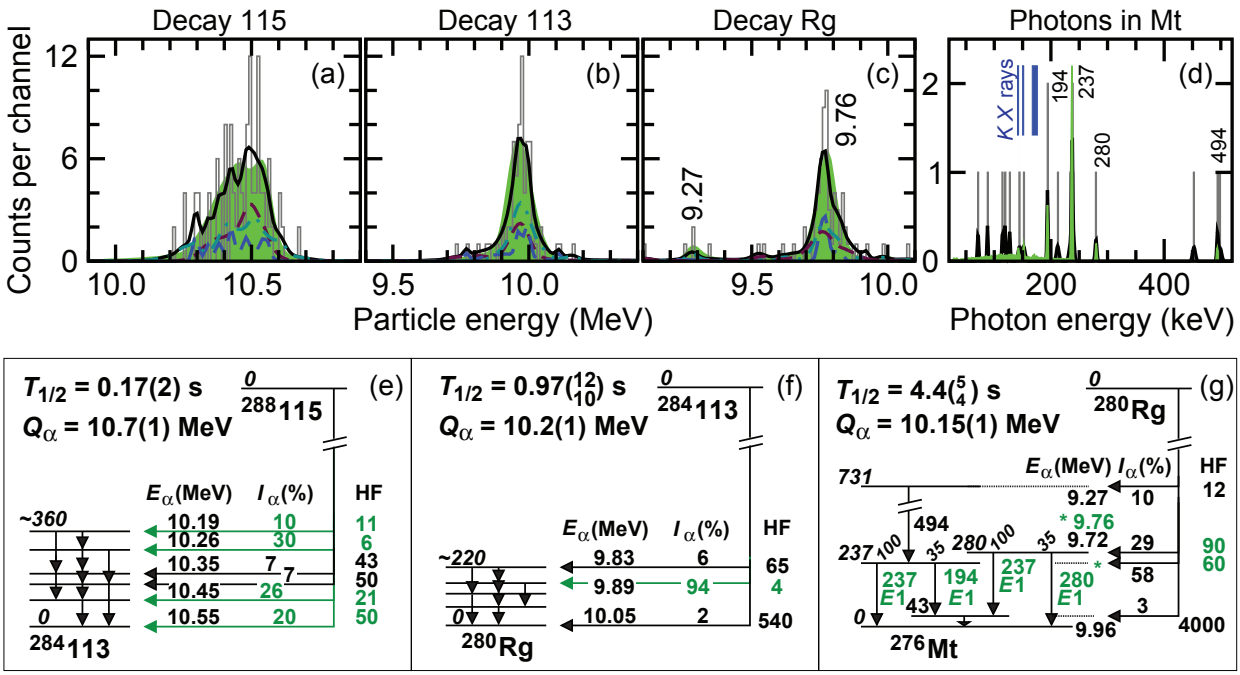

FIGURE 2. (Color online) Panels (a)-(d) are particle- and photon-energy spectra of the first three steps of decay chains associated with ^{288}115. The grey histograms represent the events from the combined three data ensembles (DGFRS [16], TASCA [14, 17], BGS [20]) displayed in the traditional fashion. The continuous black curves are sums of Gaussian-shaped distributions, hence taking into account the experimental mean values (cf. grey histograms) and, more importantly, the uncertainties of the individual decay-energy measurements. In the particle-energy spectra (a)-(c), the contributions from the three ensembles are also separately shown: DGFRS (dashed maroon), TASCA (long-dashed blue) and BGS (dot-dashed cyan). The blue bars in panel (d) mark the expected *K X*-ray energies for Z = 109, Mt. The green distributions in panels (a)-(d) are the results of Geant4 simulations [19, 26] using the proposed decay schemes in panels (e)-(g) as input. The main features of the decay schemes are highlighted in green.

As a consequence, the conventional way of incrementing histograms at mean energy values, i.e. the grey spectra in Figures 2(a)-(c), can be misleading, because different experiments provide different spectroscopic quality of the data. Furthermore, reconstructed events are by default some three times less accurate than full-energy events. In turn, each energy measurement can be represented by a Gaussian with given mean value and width, σ, corresponding to the uncertainty of the individual measurement. The continuous black curves in Figures 2(a)-(c) are the sums of these Gaussians for all secure data points within the in total 96 ^{288}115 chains. Note that the FWHM-type uncertainties of decay energies in Ref. [16] were divided by 2.35 to properly match 1σ-type energy uncertainties in Refs. [14, 20]. The contributions from the three ensembles to the total spectrum are consistent, with the ^{280}Rg spectrum derived from Ref. [16] shifted +20 keV to match the centroid of the spectra based on the other two spectroscopy experiments.

The decay-energy spectrum of ^{288}115 in Figure 1(a) shows a rather broad distribution between some 10.3 and 10.6 MeV. This feature is indicative for one or several α-decay branches into a number of excited states in the daughter nucleus ^{284}113, as discussed in Ref. [22] in some detail already. Remember, however, that neither correlation times (cf. Figure 1(d) and Table 1) nor energy-time correlations point to more than one decaying state of ^{288}115. Feeding the proposed decay scheme of ^{288}115 shown in Figure 2(e) into the comprehensive TASISpec Geant4 simulations [19, 26] results in the green-shaded background displayed in Figure 2(a). This normalized green distribution of 10000 simulated decay events is to be compared with the experimental black curve. Since the implantation set-ups and analysis procedures are quite similar at all three experimental facilities, the generic use of the TASISpec Geant4 simulation should not lead to any major discrepancy.

Including the most recent BGS data [20] provides a somewhat more detailed decay scenario compared with the one discussed in Ref. [22], while the derived Q_α = 10.7(1) MeV remains unchanged. To account for the full width of the observed experimental energy distribution, the extended decay scenario requires significant feeding at about 300 keV excitation energy as well as near the ground state of ^{284}113. The former ~ 40 % yield a hindrance factor

of about HF ~ 10 (calculated according to Equation 12 in Ref. [24]) and the latter ~ 45 % give HF ~ 35, similar to the anticipated weak α feeding at some 150-200 keV excitation energy. All excited states are set to cascade down by highly-converted low-energy $M1$ and $E2$ transitions, as there are hardly any α-photon coincidences observed for this decay step [14, 20]. Half-life, Q_α value, coarse feeding pattern and hindrance factors are the rather well-defined *gross features* of the observed ^{288}115 decay, re-affirmed by the Geant4 simulations. Details such as 'exact' α-decay or γ-ray branching ratios or energies and number of excited states remain unknown.

The situation is comparable but simpler for the decay of ^{284}113. Also in this case, there is no apparent evidence for more than one decaying state, which is defined as the ground state of ^{284}113. The experimental decay-energy distribution of Figure 2(b) is broader (FWHM ~ 90 keV) than expected for a single α-decay line (FWHM ~ 30-40 keV including reconstructed events), but certainly less broad than the one discussed for ^{288}115. The main feature of the ^{284}113 decay displayed in Figure 2(f) is a favoured E_α ~ 9.9-MeV decay into a state in ^{280}Rg at ~ 150 keV excitation energy, cascading to the ground state by multiple highly-converted $M1$ and $E2$ transitions. Small α-decay branches of about 5 % into one or several higher-lying states and the ground state are necessary to include in the Geant4 simulation, the latter due to a few full-energy energy events in excess of E_α = 10 MeV.

The decay of ^{280}Rg is the one most relevant for nuclear structure assessments. Based on only six photon events observed *in coincidence* with E_α ~ 9.76 MeV and supported by Geant4 simulations, two $E1$ transitions at 194 and 237 keV were postulated in the daughter ^{276}Mt [14] – and to some surprise, only a very limited number of single-particle Nilsson orbitals are available, which can explain the observation of these $E1$ transitions [27]. Though having worse energy resolution, the BGS data provided 15 more α-photon *coincidence events*, including four consistent with 9.76 MeV-237 keV, one at 9.75(2) MeV-279.6(16) keV, and one at 9.28 MeV-494.2(13) keV [20]. The combined photon spectrum is shown in Figure 2(d) as histogram (grey), sum of Gaussians (black), and the result of a Geant4 simulation (green). The latter refers to the decay scheme shown in Figure 2(g). It is normalized according to the α-decay spectrum of Figure 2(c).

The most important result of the combined data sets is the rock solid presence of a 237-keV $E1$ transition in ^{276}Mt. Once more, some details of the ^{280}Rg decay scheme can be discussed, such as the suggestion of two different 237-keV transitions or the 'exact' α-decay branching ratios into the 237- and 280-keV states in ^{276}Mt. Nevertheless, the presence of a ~ 10 % feeding into the high-lying state at 731 keV, introduced in Ref. [20], can be considered firm due to an additional photon at ~ 494 keV [20] and one or another additional particle-decay energy observed at ~ 9.27 MeV [14, 20]. This branch is also physically sound due to a relatively low hindrance factor. Similarly, there are a number of particle-decay events close to 10 MeV in the combined data, which point towards direct but small feeding of the low-lying level at 43 keV or the ground state. Hindrance factors of a few thousand are the consequence. This is consistent with α decays involving a change of parity, completely in line with the parity changing $E1$ transitions. The total conversion coefficient of ~ 200 keV $E1$ transitions in Z = 109, Mt, is α_{tot} ~ 0.1. With 2+6+1=9 $E1$ counts, one expects to observe also one K_α X ray in the experimental spectrum of Figure 2. Indeed, two candidates are present in the BGS data [20], while a firm X-ray identification of element 115 decay chains at this step is hampered by the Compton background of the $E1$ γ rays [cf. discussion in Ref. [20] and Geant4 simulation in Figure 2(d)].

SUMMARY AND OUTLOOK

Modern spectroscopy tools in conjunction with significant feedback from comprehensive Geant4 simulations provide first glimpses of solid experimental information for detailed nuclear structure assessments of the heaviest atomic nuclei available today. For instance, experimental facts such as the presence of 200-300-keV $E1$ transitions in ^{276}Mt must be accounted for by any nuclear structure model or model parametrization claiming relevance for superheavy element structure [27]. Furthermore, comparisons of theoretical predictions with experimental data on odd-mass or odd-odd isotopic chains should go beyond generic Q_α considerations based on nuclear masses at a given deformation (see, e.g., Refs. [28, 29, 30]), but reflect upon measured hindrance factors and connect to underlying single-particle states (e.g., Refs. [27, 31, 32, 33]), eventually corrected for particle-rotor or two-quasiparticle plus rotor effects.

For instance, the ^{287}115 chain (cf. Table 1) reveals small hindrance factors of HF ~ 4, 2, 30, 20, 10 all the way to ^{267}Db, which for sure are *not* consistent with simply connecting the lowest predicted single-particle states listed in, e.g., Refs. [27, 32, 33]. Instead, adding a particle-rotor scheme on top of a macroscopic-microscopic approach [34] suggests the following picture, which is consistent with these favoured or only slightly disturbed hindrance factors: the ^{287}115 decay chain starts with the odd 115th proton occupying the $f_{5/2}$ orbital (or [521]1/2 Nilsson orbital) near spherical shape, just above a possible Z = 114 shell gap. Along the five steps of the chain, the downsloping [521]1/2 orbital is crossed by exactly five upsloping Nilsson orbitals while deformation increases more or steadily to ε_2 ~ 0.2.

Hence, in this interpretation the odd proton *remains* in its original [521]1/2 Nilsson single-particle state, because for each decay step the $J = 0$ proton pair in the respective upsloping Nilsson orbital can be readily taken to form the emitted α particle. Minor hindrance can occur due to shape changes and/or some Coriolis mixing.

On the experimental side, high-class spectroscopic α-photon coincidence information on odd-A neighbours of ^{276}Mt is required to pin down the origin of the observed $E1$ transitions. This can be done by exploring even-Z-odd-N chains starting from ^{285,287}Fl or ^{289}Lv, likewise probing more odd-Z-even-N ^{287}115 chains. The situation is unclear for ^{289}115 [17]. In general, the production yields for all these decay chains as well as other interesting odd-A or odd-odd cases are lower by a factor of about three. To obtain reasonable statistics of high-quality spectroscopic data, this decrease needs to be compensated either by prolonged beam times or, preferably, by increased primary beam currents in conjunction with further optimized decay stations.

ACKNOWLEDGMENTS

NSD 2015 attendance and these Proceedings are supported by the Swedish Research Council and the Royal Physiographic Society in Lund. The assembly of TASISpec would have been impossible without generous grants from the Royal Physiographic Society in Lund and support from the Euroball Owners Committee. The GSI experiment on element 115 was supported by the European Community FP7 – Capacities ENSAR No. 262010.

REFERENCES

[1] M. Schädel, Phil. Trans. R. Soc. A **373**, 20140191 (2015).
[2] S.G. Nilsson *et al.*, Nucl. Phys. **A131**, 1 (1969).
[3] M. Bender, W. Nazarewicz, and P.-G. Reinhard, Phys. Lett. **B515**, 42 (2001).
[4] S. Ćwiok, P.H. Heenen, and W. Nazarewicz, Nature **433**, 705 (2005).
[5] J. Dvorak *et al.*, Phys. Rev. Lett. **97**, 242501 (2006).
[6] R.-D. Herzberg and P.T. Greenlees, Prog. Part. Nucl. Phys. **61**, 674 (2008).
[7] Y.T. Oganessian, J. Phys. G **34**, R165 (2007); Radiochim. Acta **99**, 429 (2011).
[8] Y.T. Oganessian *et al.*, Phys. Rev. C **87**, 054621 (2013).
[9] R.C. Barber *et al.*, Pure Appl. Chem. **83**(7), 1485 (2011).
[10] G.T. Seaborg and W.D. Loveland, *The Elements Beyond Uranium* (Wiley-Interscience, New York, 1990).
[11] C.E. Bemis, Jr. *et al.*, Phys. Rev. Lett. **31**, 647 (1973).
[12] T.A. Carlsson *et al.*, Nucl. Phys. **A135**, 57 (1969); At. Data Nucl. Data Tables **19**, 153 (1977).
[13] H.G.J. Moseley, Phil. Mag. **26**, 1024 (1913).
[14] D. Rudolph *et al.*, Phys. Rev. Lett. **111**, 112502 (2013).
[15] Yu. Ts. Oganessian *et al.*, Phys. Rev. C **69**, 021601(R) (2004).
[16] Yu. Ts. Oganessian *et al.*, Phys. Rev. C **87**, 014302 (2013).
[17] U. Forsberg *et al.*, submitted to Nucl. Phys. A; http://arxiv.org/abs/1502.03030.
[18] L.-L. Andersson *et al.*, Nucl. Instrum. Meth. A **622**, 164 (2010).
[19] L.G. Sarmiento, L.-L. Andersson, D. Rudolph, Nucl. Instrum. Meth. A **667**, 26 (2012).
[20] J.M. Gates *et al.*, Phys. Rev. C, in press.
[21] D. Rudolph *et al.*, Acta Phys. Pol. **B45**, 263 (2014).
[22] D. Rudolph *et al.*, J. Radioanal. Nucl. Chem. **303**, 1185 (2015).
[23] D. Rudolph *et al.*, JPS Conf. Proc. **6**, 010026 (2015)
[24] C. Qi *et al.*, Phys. Rev. C **80**, 044326 (2009).
[25] K.-H. Schmidt, Eur. Phys. J. A **8**, 141 (2000).
[26] L.G. Sarmiento *et al.*, Proceedings of Science, PoS(X LASNPA)057 (2014).
[27] Yue Shi *et al.*, Phys. Rev. C **90**, 014308 (2014).
[28] Hongfei Zhang *et al.*, Phys. Rev. C **71**, 054312 (2005).
[29] A. Sobiczewski, Phys. Scr. **89**, 054014 (2014).
[30] A. Sobiczewski, Acta Phys. Pol. **B46**, 551 (2015).
[31] S. Ćwiok, W. Nazarewicz and P.H. Heenen, Phys. Rev. Lett. **83**, 1108 (1999).
[32] A. Parkhomenko and A. Sobiczewski, Acta Phys. Pol. **B35**, 2447 (2004).
[33] A. Parkhomenko and A. Sobiczewski, Acta Phys. Pol. **B36**, 3115 (2005).
[34] I. Ragnarsson, private communication.